Article

Extracting Taklimakan Dust Parameters from AIRS with Artificial Neural Network Method

Zhigang Yao [1,2], Jun Li [3], Zengliang Zhao [1], Lin Zhu [4], Jin Qi [4,*] and Huizheng Che [5]

[1] Beijing Institute of Applied Meteorology, Beijing 100029, China; zhigangyao@mail.iap.ac.cn (Z.Y.); zzl@pku.org.cn (Z.Z.)
[2] LAGEO, Institute of Atmospheric Physics, Chinese Academy of Sciences, Beijing 100029, China
[3] Cooperative Institute for Meteorological Satellite Studies (CIMSS), University of Wisconsin-Madison, Madison, WI 53706, USA; jun.li@ssec.wisc.edu
[4] National Satellite Meteorological Center, Beijing 100081, China; zhulin@cma.gov.cn
[5] Key Laboratory of Atmospheric Chemistry (LAC), Chinese Academy of Meteorological Sciences, Beijing 100081, China; chehz@cma.gov.cn
* Correspondence: qijin@cma.gov.cn

check for updates

Abstract: Two back-propagation artificial neural network retrieval models have been developed for obtaining the dust aerosol optical depth (AOD) and dust-top height (DTH), respectively, from Atmospheric InfraRed Sounder (AIRS) brightness temperature (BT) measurements over Taklimakan Desert area. China Aerosol Remote Sensing Network (CARSNET) measurements at Tazhong station were used for dust AOD validation. Results show that the correlation coefficient of dust AODs between AIRS and CARSNET reaches 0.88 with a deviation of −0.21, which is the same correlation coefficient as the AIRS dust AOD and the Moderate-Resolution Imaging Spectroradiometer (MODIS) aerosol optical depth (AOD) product. In the AIRS DTH retrieval model, there is an option to include the collocated MODIS deep blue (DB) AOD as additional input for daytime retrieval; the independent dust heights from Cloud-Aerosol Lidar with Orthogonal Polarization (CALIOP) are used for AIRS DTH validation, and results show that the DTHs derived from the combined AIRS BT measurements and MODIS DB AOD product have better accuracy than those from AIRS BT measurements alone. The correlation coefficient of DTHs between AIRS and independent CALIOP dust heights is 0.79 with a standard deviation of 0.41 km when MODIS DB AOD product is included in the retrieval model. A series of case studies from different seasons were examined to demonstrate the feasibility of retrieving dust parameters from AIRS and potential applications. The method and approaches can be applied to process measurements from advanced infrared (IR) sounder and high-resolution imager onboard the same platform.

Keywords: dust aerosol optical depth; dust top height; retrieval; AIRS; MODIS

1. Introduction

Understanding spatial and temporal distributions of dust height and optical depth is of great importance to dust monitoring, warnings, as well as forecast and climate change research [1–3]. Central Asia, including northwest China, is one of four areas in the world with the most dust storms (the other areas are the southwestern area of North America, North Africa, and Australia). The land cover of this region is mainly sparse vegetation and crumbly soil with rich mineral particles [4]. As a result, sandstorms may occur at any time when certain weather conditions are met [5]. Previous research has noted that dust storms in this region not only influence the atmospheric environment [6,7] but also significantly impact marine ecosystems by transporting the iron-containing soil and further affecting

the global climate [8–11]. In addition, aerosols in the Northwest Pacific Ocean have a close relationship with dust storms in East Asia [12].

The Taklimakan Desert is one of the main sources of sandstorms in the world, with sandstorms occurring in this area both day and night [13]. Due to the severe natural environment in this region, there are only a limited number of observation stations. The spatial and temporal distribution and strength of the sandstorms often vary in an inhomogeneous way, making it impossible to acquire three-dimensional variations of the sandstorm using conventional observation methods. Measurements from satellite-based high spectral resolution infrared (IR) atmospheric sounders [14] can be used to monitor and estimate dust height and dust aerosol optical depth (AOD) in this area. Compared with station observations, satellite technology becomes a more effective way to monitor dust weather. However, it is still difficult to estimate dust-top height (DTH) and night time dust AOD from a satellite-based passive and spectral imager with moderate spatial resolution such as the Moderate-Resolution Imaging Spectroradiometer (MODIS). For instance, although satellite-based thermal IR observations can be used to detect dust storms and retrieve optical depth of dust storms [15–17], it is difficult to obtain height information. For shortwave bands, it is difficult to acquire accurate dust AOD over areas with high surface albedo [18]. The daytime dust AOD can be derived from the Deep Blue (DB) method [19] based on satellite data under a bright land surface background. However, the DB method cannot be used to acquire DTH and dust AOD at night. In addition, although active remote sensing data such as CALIOP (Cloud-Aerosol Lidar with Orthogonal Polarization) can be used to estimate the vertical structure of dust storms, only nadir observation is available. Therefore, it is not suitable for broad-range dust monitoring.

Dust and meteorological clouds show different signals when observed by satellite-based high spectral infrared sensors such as the Atmospheric InfraRed Sounder (AIRS). Therefore, these sensors can be used to extract dust optical depth and height not only for daytime but also for nighttime [20,21]. Pierangelo et al. [22] developed a look-up table method based on precalculated data, from which AIRS is used to retrieve dust-top height (DTH) and infrared optical depth over the Atlantic. De Souza-Machado et al. [23] analyzed dust infrared signals over the ocean using AIRS infrared observations; due to higher emission and variation, it is more difficult to estimate dust AOD and DTH over land than that over the ocean [24]. Yao et al. [25] analyzed the feasibility of retrieving DTH and optical depth over land using AIRS with a 1Dvar-based iterative method. With infrared land surface emissivity (LSE) and atmospheric profile data as ancillary input data, the DTHs, along with the dust AODs over land were derived from AIRS BT measurements, and results show the great potential of AIRS in the retrieval of dust parameters. Han and Sohn [26] developed a statistical model based on collocated AIRS BT measurements, MODIS AOD product, and CALIOP dust height observations. Yao et al. [27] also analyzed the feasibility of retrieving DTH using combined AIRS BT measurements and MODIS DB product and got some preliminary results. Overall, these previous studies mainly focused on limited observation data. It is still necessary to further analyze the properties of dust aerosol over an area with high-frequency dust events.

The main purposes of this study are to develop statistical models suitable for dust AOD and DTH retrieval from AIRS BT measurements and to calculate the statistics of the averaged DTH near the dust source regions, which is useful for understanding and modeling of dust origination and transportation. This study is different from previous research in the following aspects: (1) in-situ measurements are used to validate dust AOD products derived from AIRS; (2) the influence of MODIS DB AOD on AIRS DTH retrieval is investigated and evaluated; and (3) the method and approaches are established and now can be applied to process measurements from an advanced IR sounder and a high-resolution imager onboard the same platform, such as the Cross-track Infrared Sounder (CrIS) and the Visible Infrared Imaging Radiometer Suite (VIIRS) onboard the Suomi-NPP platform and JPSS (Joint Polar Satellite System) series. With the developed algorithms and technical approached, real-time continuous dust monitoring from a hyperspectral IR sounder onboard a geostationary platform such as GIIRS (Geosynchronous Interferometric Infrared Sounder, onboard the Fengyun-4 series [28]) is now possible.

Independent typical case studies have been conducted in order to demonstrate the application of the statistical retrieval models, as well as to evaluate the performance of AIRS dust retrievals. Section 2 describes the data used in this study; Section 3 describes the algorithms and technical approaches used for AIRS dust retrieval; Section 4 presents various case studies along with DTH retrievals; Section 5 presents DTH statistics over the Taklimakan Desert; Section 6 presents the discussion about method and results; conclusion is summarized in Section 7.

2. Data

2.1. AIRS

AIRS is a hyper-spectral resolution infrared instrument onboard the Aqua satellite as part of the A-train, launched on May 4, 2002 [29]. AIRS has 2378 channels covering the wavelength range of 3.7–15.4 microns, with a spatial resolution of 13.5 km at nadir. AIRS was designed to support climate research and improve weather forecasting by retrieving atmospheric temperature, water vapor, and trace gases with a 2000 km swath. Its measurements are also sensitive to dust atmospheric and could extract quantitative information [22–25]. In this study, AIRS Level-1B BT measurements over Taklimakan Desert area ([35°N, 45°N, 75°E, 95°E]) have been collected. The data from 2007 to 2013 were used for the statistical model developing and validation. For independent validation, the retrieved AIRS dust AOD with the in-situ observations, AIRS L1B data from 2004 to 2009 were collected and processed.

2.2. MODIS

MODIS instrument onboard Aqua satellite has 36 spectral bands ranging in wavelength from 0.4 um to 14.4 um with a high spatial resolution and a near-daily global coverage. Hsu et al. [19] used the MODIS DB algorithm, employing two lower reflective bands (412 nm and 470 nm) to retrieve AOD properties over the drought area. The AOD properties were validated with AERONET observations over China and Outer Mongolia, in which the uncertainty of the MODIS DB products ranged from 20 to 30% [30]. Li et al. [31] evaluated MODIS DB products using AOD data measured by the sun photometer acquired from four stations in the Xinjiang province during 2002 and 2003. Results showed that the correlation coefficient between the DB products and field measurements approaches 0.94. In this work, the MODIS true-color composite images are used for demonstrating area sandstorms. The 550 nm AOD from the MYD04 (C5, spatial resolution is 10 km) DB product is used as reference data to provide dust weather information for retrieval and validation over Taklimakan Desert during 2007–2013.

2.3. CALIOP

CALIPSO (Cloud-Aerosol Lidar and Infrared Pathfinder Satellite Observations) is one of the A-Train satellite series launched by the National Aeronautics and Space Administration (NASA) on April 28, 2006. It provides a way to detect and quantify dust height. CALIOP, a lidar instrument onboard CALIPSO, provides unique global scale vertical profiles of clouds and aerosols [32]. CALIOP acquires vertical profiles of elastic backscatter at two wavelengths (532 and 1064 nm) from a near-nadir viewing geometry during both day and night. The CALIOP Level 1 product is used to obtain total attenuated backscatter at 532 nm and surface height information in the following study. For aerosols, the CALIOP Level 2 layer product exhibits the typical horizontal intervals of 5 km providing the position and optical depth of aerosol layers. The CALIOP L1 and L2 aerosol layer products were collected the same time and area as MODIS data.

2.4. CARSNET

In order to observe and study the atmospheric aerosol properties of China, the China Meteorological Administration (CMA) has developed a nationwide observation network called the China Aerosol Remote Sensing Network (CARSNET). CARSNET uses a CE318 type sunphotometer to retrieve

atmospheric aerosol optical properties by measuring narrowband solar radiation, the same instrument used by AERONET [33,34]. The AOD products of CARSNET at 440, 670, 870, and 1020 nm have been applied to support validation of the satellite retrievals and to study the climate effect of aerosols [35,36].

In this study, CARSNET observations from Taklimakan Desert stations (location: 51747, 39.00°N, 83.40°E, Tazhong site) during 2004–2009 were used to evaluate AIRS dust AOD retrievals.

3. Method and Result

3.1. Dust Detection

Designed to measure atmosphere and cloud parameters [29], AIRS can be used to detect day and night dust properties using its longwave infrared channels [21]. Previous studies have demonstrated that dust shows an absorption peak at 10 μm (1000 cm^{-1}), while ice crystals peak at 12 μm (800 cm^{-1}). DeSouza-Machado et al. [24] used 5 AIRS channels at 822.4 cm^{-1}, 900.3 cm^{-1}, 961.1 cm^{-1}, 1129.0 cm^{-1}, and 1231.3 cm^{-1} to create 9 tests and to calculate dust score for detecting dust pixel over the ocean. This dust-detection algorithm (DDA) was used over land by doubled last two tests value with the same threshold of 380. The modified DDA is the first step of data processing to pick up the dust in AIRS radiances, and then other source data collocated to AIRS dust pixel.

3.2. Data Collocate

AIRS, MODIS, and CALIOP are all a part of A-train series satellites with different spatial resolutions. A common collocation method was used to turn MODIS and CALIOP data to AIRS pixel size by considering the distances of the center positions. The mean MODIS DB AOD value is used for collocation.

For CALIOP L2 product, there may be several layers of aerosol at each pixel. The dust and polluted dust layers are identified with the information from this aerosol pixel feature classification flag. CALIOP dust height information has been extracted with the dust layer top and bottom altitudes weighted by Aerosol Optical Thickness (AOT) of corresponding layers in order to develop and validate the AIRS dust height algorithm [26]. The column aerosol and cloud optical depth at 532 nm are used for validating the night case results.

CARSNET AOD data within 7.5 min of AIRS overpass are chosen to use for AIRS dust AOD validation at Tazhong site. For collocating the AIRS dust AOD at 550 nm, CARSNET 550 nm AOD is linearly interpolated with AOD at 440 nm and 870 nm [37].

Based on the method above, 4 collocated datasets have been structured: 1) AIRS L1B data and MODIS DB AOD for dust AOD model developing and validation; 2) AIRS L1B data, MODIS DB AOD, and CARSNET AOD for AIRS dust AOD validation; 3) AIRS L1B data, CALIOP L2 dust height, and AOD for AIRS DTH model developing and validation; 4) AIRS L1B data, MODIS DB AOD, and CALIOP L2 products for AIRS DTH model developing and validation.

### 3.3. Artificial Neural Network Method

A typical Back-Propagation (BP)-based artificial neural network (ANN) algorithm was used in this research over the Taklimakan Desert ranging from 35°N to 45°N latitude and from 75°E to 95°E longitude [38,39]. Compared with a 1Dvar-based physical retrieval method, the ANN method only depends on the matched observations and dust parameter datasets and avoids the construction of the atmospheric radiation transfer model, which also needs surface and atmospheric parameters as inputs in the retrieval. The BP ANN's learning process consists of two parts: forward propagation and backward propagation. In the forward propagation stage, input information is processed by the hidden layer's exiting function and then output into the next layer of neurons. The condition of neurons at every layer influences the next layer. If the expected output is not acquired by the output layer, then the backward propagation starts. The error signals will go back through the primary neuron's connection and modify the weight of the neuron's connection for each layer. The forward and backward processes

are iterated until the signal error reaches a limited range. Using MODIS data, Cho et al. [40] detected very thin dust aerosols over the ocean with the ANN algorithm. Similar to Yao et al. [41], a three-layer network is used in this study. The input layer has no computation function and is only used to enter the input vector. BTs of nine AIRS channels (704.7 cm^{-1}, 718.0 cm^{-1}, 1224.6 cm^{-1}, 843.9 cm^{-1}, 871.3 cm^{-1}, 965.4 cm^{-1}, 1074.5 cm^{-1}, 1228.2 cm^{-1}, and 1236.5 cm^{-1}) are used as input vector, which is similar to Peyridieu et al. [42], and surface height information from AIRS L1B data is also added as input vector. The first three channels are selected for atmosphere retrieval capabilities and the other six channels are chosen for retrieving dust height and optical depth information. In the hidden layer, there are 10 nodes and each node performs a weighted sum over all of the input values and applies a sigmoidal function to produce an output vector. In the output layer, the Purelin linear function is applied and the output vector corresponds to the retrievals such as MODIS AOD (at 550 nm) and CALIOP dust height. Generally, one dataset is used to train the network and another dataset is used to evaluate the retrievals. The AIRS collocated data is based on dust detection results from the five AIRS channels. The method, presented in Section 3.1, is used to extract dust pixels and avoid cloud influence. A detailed description of the retrieval approaches is provided in the following sections.

3.4. Dust AOD from AIRS

The statistic retrieval model of AIRS dust AOD is based on the collocated data of AIRS L1B data and MODIS DB AOD from 2007 to 2013. In the database, the nine channels BTs measurement and surface elevation from AIRS L1B data were used as input vector and the collocated MODIS AOD as the output vector. The ANN model was built with 93,261 matched pairs from 2010 to 2013, and another 37,206 matched pairs from 2007 to 2009 were used for validation.

A relationship between the AIRS BTs and MODIS AODs is established. Figure 1 shows the comparison between the dust AOD extracted from AIRS and MODIS using 37,206 independent validation samples. The AIRS dust AOD is well correlated with MODIS, with a linear correlation coefficient (R) approaching 0.88, a root mean square deviation (E) of 0.53 and a deviation (B) of 0.028, which demonstrated a good agreement between the AIRS dust AOD and MODIS AOD.
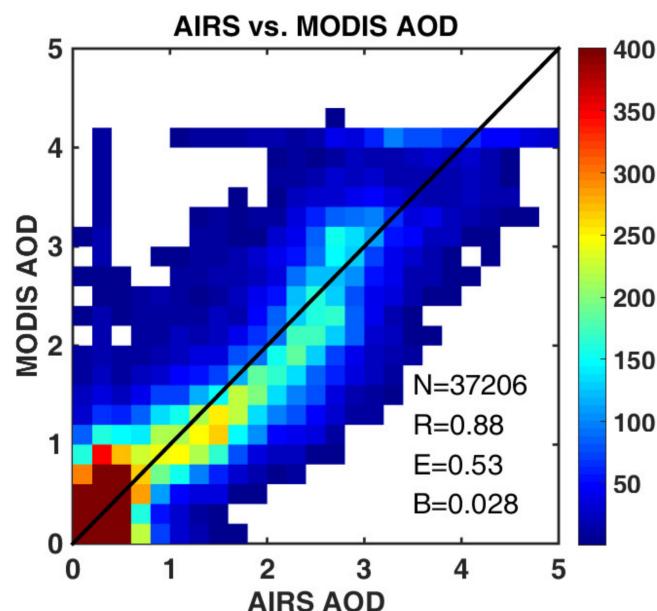
Figure 1. Comparison of the frequency distribution between dust aerosol optical depth (AOD) extracted from Atmospheric InfraRed Sounder (AIRS) and from Moderate-Resolution Imaging Spectroradiometer (MODIS) (N is the number of validation samples, R represents the relationship coefficient, E is the root mean square deviation, B represents the deviation).

In order to further test the performance of AIRS for dust AOD retrieval, matched CARSNET AOD measurements from the Tazhong site from 2004 to 2009 were used to compare and validate AIRS dust AOD. Figure 2 shows the comparison between AIRS dust AOD, MODIS AOD, and CARSNET AOD with 37 samples. The correlation coefficient (Ra) between AIRS dust AODs and CARSNET AODs is 0.88 with a deviation (Ba) of -0.21; while the correlation coefficient (Rm) between MODIS AODs and CARSNET AODs is 0.85 with a deviation (Bm) of -0.26. The results suggest that AIRS and MODIS have similar abilities in retrieving dust aerosol optical depth. Generally, when the AOD is less than 1, the satellite-derived AOD tends to be underestimated. However, the above results demonstrate that AIRS is applicable for extracting dust AOD over land.
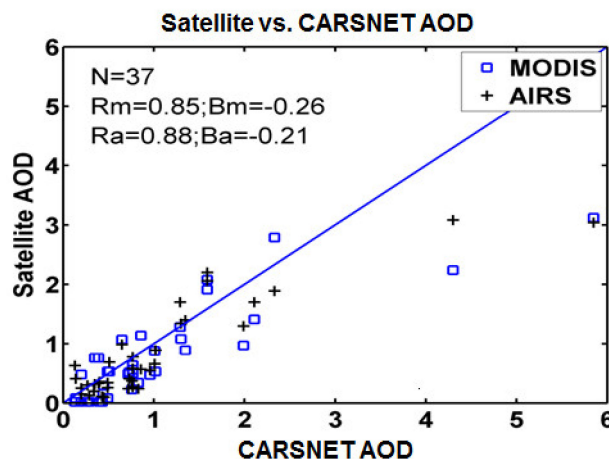
Figure 2. Scatter plot showing satellite-derived AOD (AIRS and MODIS) and China Aerosol Remote Sensing Network (CARSNET) field measurements (central location: 51747, 39.00°N, 83.40°E, Tazhong site) from 2004 to 2009 (N is the number of samples, Rm and Bm are the correlation coefficient between MODIS AOD and CARSNET AOD and corresponding deviation; Ra and Ba are the correlation coefficient between AIRS AOD and CARSNET AOD and corresponding deviation).

3.5. DTH from AIRS

The statistic retrieval model of AIRS DTH is firstly based on the collocated data of AIRS L1B data and CALIOP L2 dust height which has matched to AIRS pixel with the weighted-average method from 2007 to 2013 [26]. The dust DTH model is developed similarly as dust AOD model. In order to reduce the influence of dust layer below atmospheric boundary layer, the mean height of a single dust layer which was 1 km higher than the land surface is used to compute the CALIOP weighted dust height. Furthermore, the dust layer that is higher than 6 km is excluded to reduce the influence of cirrus clouds. With the improved collocation database, 466 matched samples were acquired using satellite observations between 2007 and 2013, from which 366 samples with an early observation time were used to train and develop a statistical retrieval model for DTH, while the other 100 independent samples were used for validation. It is worth examining that relatively strict principles were used to construct the matchup database in order to reduce the influence of other factors. As a result, the number of final matched samples is not very large.

Observations from multiple instruments onboard the same platform can be used together for cloud and dust retrievals [27,43,44]. According to the simulation experiments conducted by Yao et al. [27], the retrieval error of the DTH could be reduced by combining MODIS DB AOD and AIRS BT measurements. The DTH error is less than 0.5 km when the DTH is greater than 2.0 km and the MODIS DB AOD is greater than 0.5. Therefore, MODIS DB AOD was used as one of the input parameters, and a DTH retrieval model was established using AIRS BT measurements with an option of including MODIS DB AOD as input for daytime retrieval.

Figure 3 shows the validation results for AIRS DTH retrievals. AIRS DTHs and CALIOP dust heights have a close relationship, in which R is equal to 0.79 and the deviation is equal to 0.41 km.

The results demonstrate that AIRS is feasible for DTH retrieval. A nine-channel retrieval model based on AIRS BT measurements was further established for analyzing the influence of MODIS DB AOD on the DTH retrieval. If only AIRS BT measurements were used, the correlation coefficient between retrievals and CALIOP dust heights is 0.75 and the deviation is 0.44 km, indicating that adding MODIS DB AOD information can significantly improve the accuracy of AIRS DTH retrievals. However, for nighttime retrievals, only the AIRS nine-channel BT measurements are used.
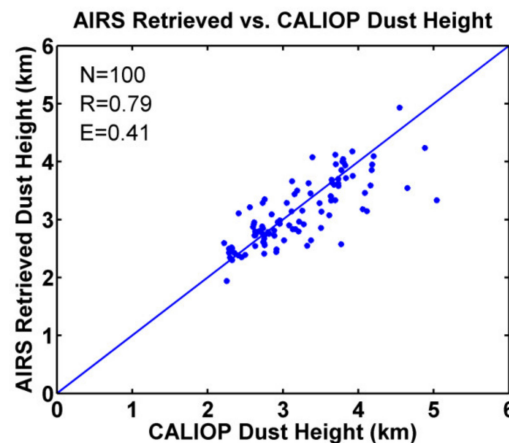

Figure 3. Scatter plot showing AIRS dust height and Cloud-Aerosol Lidar with Orthogonal Polarization (CALIOP) observations (N is the number of matched samples, R is the correlation coefficient and E is the deviation).

4. Case Studies

A series of case studies for different seasons and dust strengths were examined to further analyze the feasibility of AIRS for DTH retrieval. CALIOP vertical profiles were used to compare with satellite extracted DTH results. The study periods are April 4, 2013, November 11, 2013, and March 19, 2010. The first two case studies, conducted during the daytime, are located in the Taklimakan Desert while the last case study, conducted at night, is located in the Gadain Jaran Desert and its neighboring district. Dust AOD was derived from the statistical model using AIRS BT measurements, as described in Section 3. For the daytime DTH retrieval, the retrieval model uses both AIRS BT measurements and MODIS DB AOD product, while for the nighttime DTH retrieval, the retrieval model uses only AIRS BT measurements. It should be noted that since the nine AIRS channels also contain both the surface and atmospheric profile information, the statistical retrieval model is able to take into account the surface and atmospheric profile effect in the DTH retrieval.

4.1. Case 1: April 4, 2013

Figure 4a is a visible image acquired by MODIS at 15:55 (local time) on April 4, 2013. It shows that most of the Taklimakan Desert was covered by dust. Heavier dust was observed in the northwest, central, and northern areas. Near the surface, winds were from the northwest according to the dust report from the China Meteorological Administration (CMA). Figure 4b shows the dust AOD retrievals from AIRS BT measurements. The retrieved dust distribution indicates agreement with the visible image. The dust area had a higher corresponding retrieved dust AOD than the surrounding area.
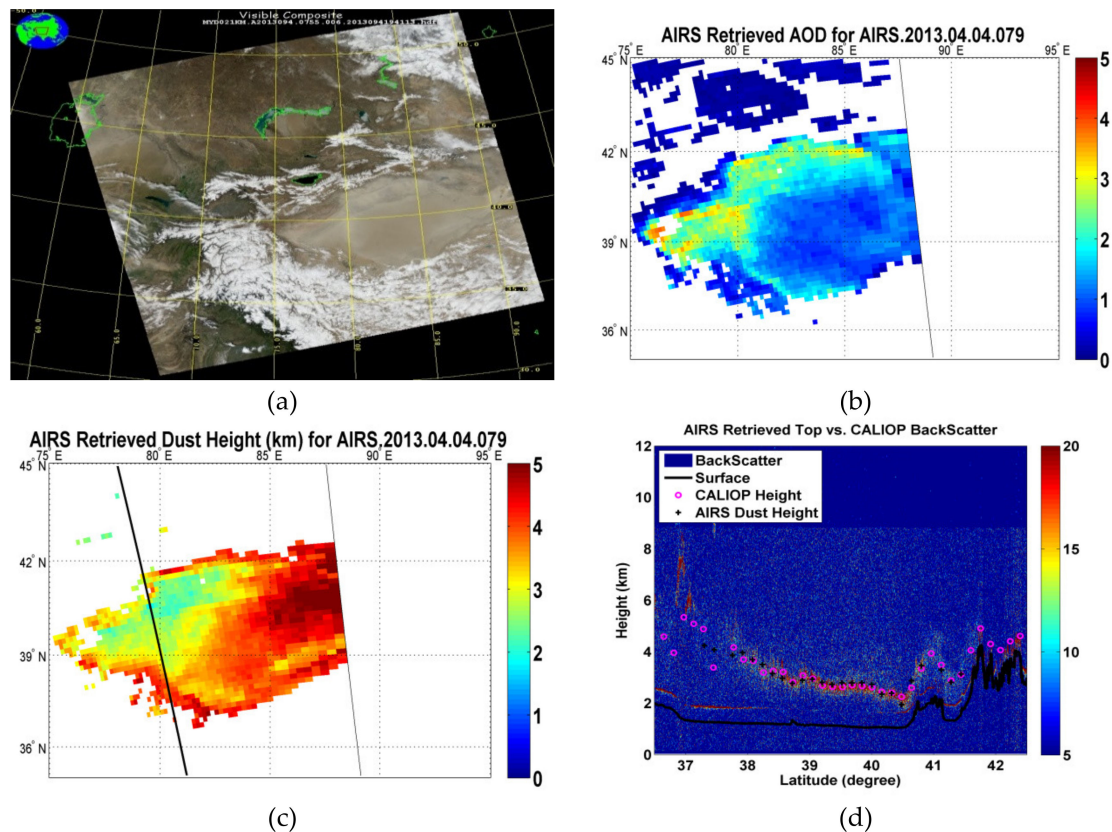
Figure 4. Comparison of AIRS retrievals and CALIOP observations (April 4, 2013). (**a**) Visible image acquired by MODIS at 15:55 on April 4, 2013 (local time), (**b**) dust AOD extracted from AIRS observations, (**c**) dust height in unit of km derived from AIRS and CALIOP track indicated by black line, (**d**) comparison of AIRS dust height and CALIOP observation. The backscatter in unit of $km^{-1}sr^{-1}$ is multiplied by 1000, the surface height in unit of km by black line, the CALIOP dust height in pink circle, the AIRS DTHs in black crosses.

The extracted DTHs are displayed in Figure 4c. The DTHs in the northwest area are about 2 km, while in the east, the DTH increases to 5 km. The total attenuated backscatter at 532 nm of the atmospheric vertical profile observed by CALIOP along its observation track is shown in Figure 4d. The color bar shows the backscatter (km-1 sr-1) times 1000. Pink circles represent CALIOP dust heights and black crosses represent AIRS DTHs. The dust heights from CALIOP are determined by the method described in Section 3.2. From 37°N to 40.5°N latitude, the dust heights are gradually reduced from 5 km to 2 km. While from 40.5°N to 41.5°N latitude, the CALIOP dust heights are first increased and then decreased due to topographic effects. These variations are fairly reflected in the AIRS DTH retrievals. Therefore, it can be concluded that there is good agreement between AIRS DTH retrievals and CALIOP dust height observations.

4.2. Case 2: November 11, 2013

As shown in Figure 5a, a strong sandstorm covering most of the Taklimakan Desert was observed on November 11, 2013. The strongest dust occurred at the eastern entrance to the desert while dust in other areas was relatively weak. The distribution of AIRS-derived dust AODs (Figure 5b) agrees well with the satellite visible image, with the largest dust AODs up to 3; from the AIRS derived DTH image, it can be seen that the DTHs in the heavier dust areas are 2–3 km (Figure 5c). From the comparison between CALIOP and AIRS (Figure 5d), the dust heights extracted from CALIOP range from 2 to 3 km. At 40.8°N, the CALIOP dust heights are relatively low, while there is a high value at 41.5°N

due to an orographic influence. The AIRS DTHs accurately capture the variations of dust heights from CALIOP.
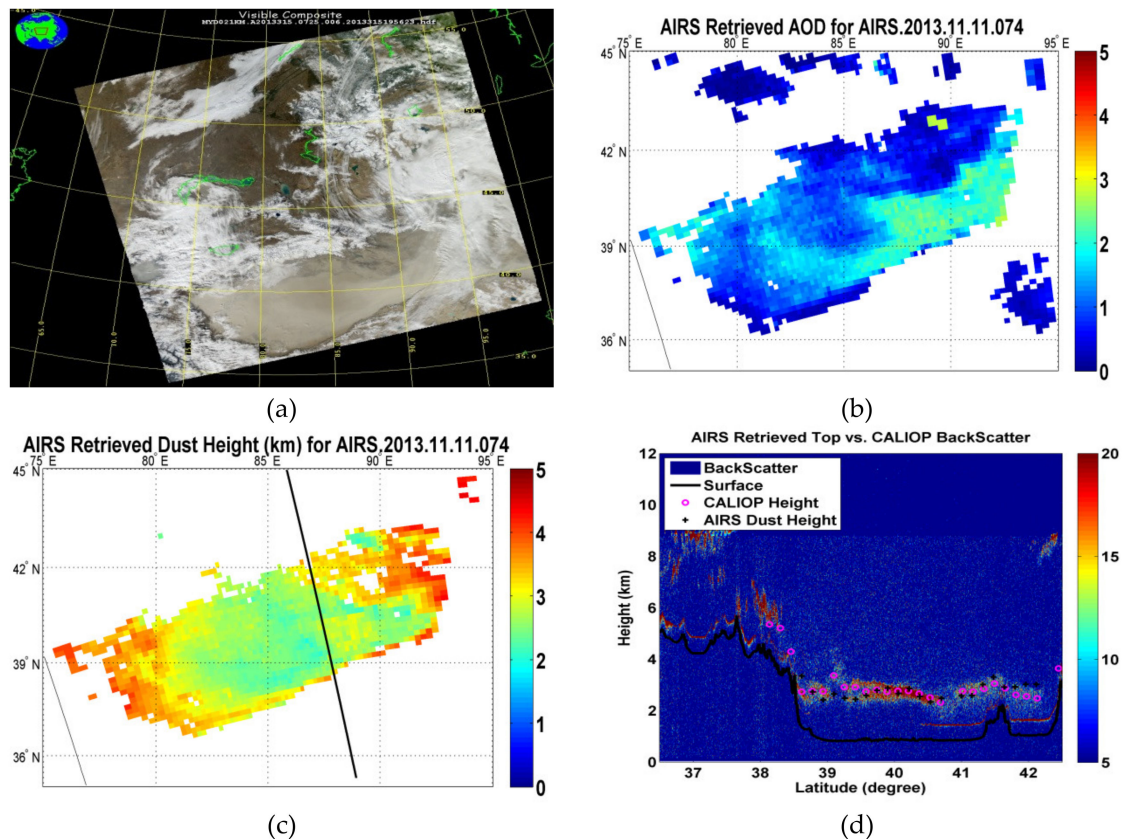
Figure 5. Comparison of AIRS retrievals and CALIOP observations (November 11, 2013). (**a**) Visible image acquired by MODIS at 15:25 on November 11, 2013 (local time), (**b**) Dust AOD extracted from AIRS observations, (**c**) Dust height derived from AIRS and CALIOP track indicated by black line, (**d**) Comparison of AIRS dust height and CALIOP observation, same as Figure 4.

4.3. Case 3: March 19, 2010

In the two cases above, the DTH retrieval results were derived and demonstrated for the daytime. While nighttime applications of the above statistical models still pose a challenge, it is worth examining the feasibility of applying daytime training data to nighttime cases. Wang et al. [13] suggested that the frequency of dust storms occurring at nighttime is relatively low, as most occur during the daytime. Considering that the Aqua overpass times are at 1:30 and 13:30 (local time), it is difficult to acquire matched data at night. A case study in the Hexi area on March 19, 2010, as shown in Figure 6, is presented here. The 11 um infrared BT image (Figure 6a) indicates a low cloud temperature (lower than 240 K). In the northeast of this cloud, a large area of dust was detected spreading from the north-central to the southeastern part of the Badain Jaran Desert. The AIRS-derived dust AODs show that the dust over southeast of the desert is relatively thick (dust AOD is about 3), while over the central and northern portions of the desert, the dust AOD value is about 2. Looking at the CALIOP-derived dust AODs, over the area between 38.5°N and 40°N, the CALIOP AODs first increase and then decrease, which is similar to the variations in the AIRS dust AODs, and also with comparable AOD values. CALIOP dust heights and AIRS DTHs are in good agreement over this area with values around 4 km. Over the area between 38°N and 40°N latitude, the CALIOP dust heights increase first and then decrease, which is similar to the AIRS DTHs, ranging between 3 and 4 km.
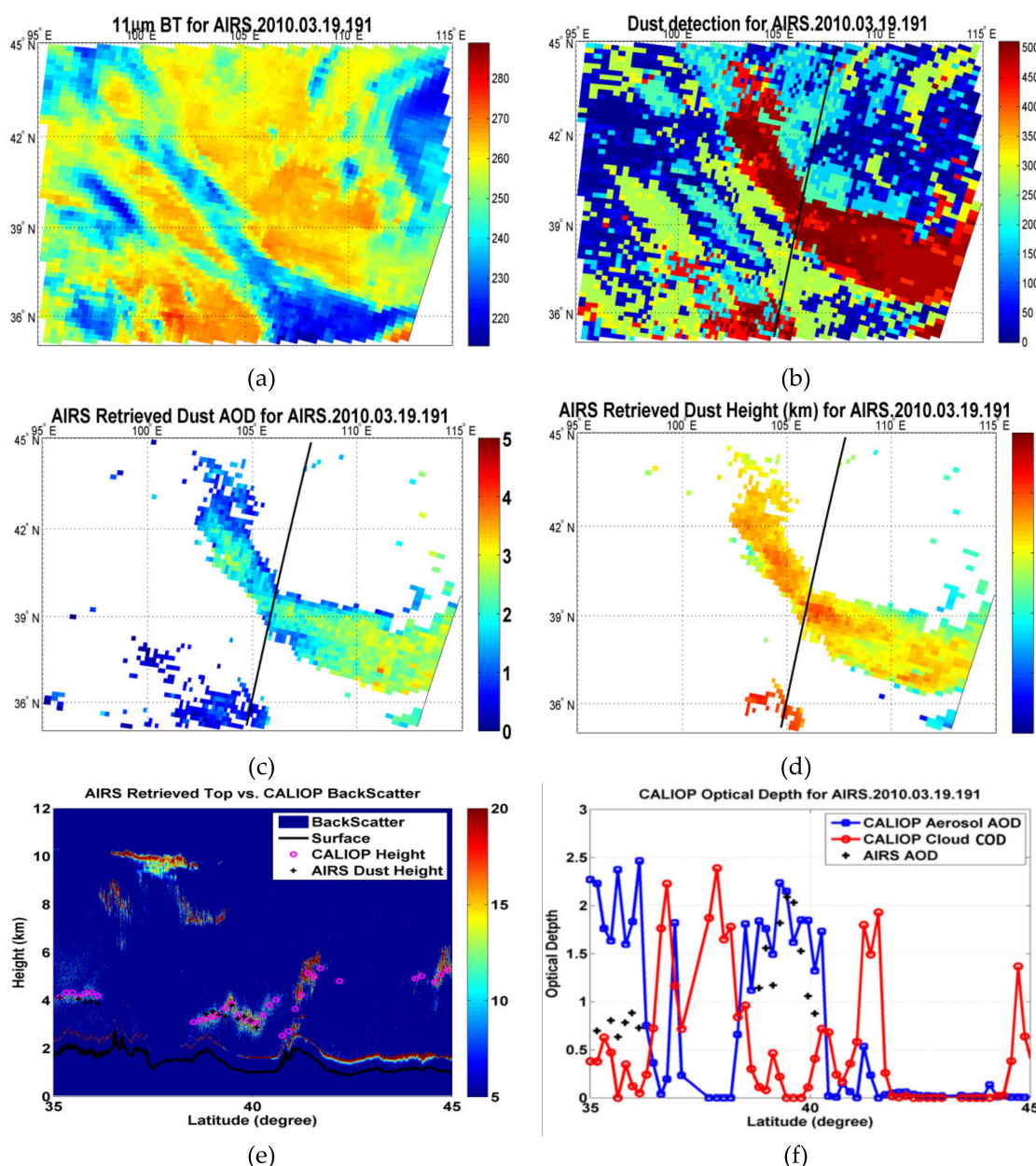
Figure 6. Comparison of AIRS-derived dust parameters and CALIOP observations products (March 19, 2010). (**a**) Infrared brightness temperature observed by AIRS, (**b**) Dust score derived from AIRS and CALIOP track indicated by black line, (**c**) Dust AOD derived from AIRS, (**d**) Dust height in unit of km derived from AIRS, (**e**) Comparison of AIRS dust height and CALIOP observations, same as Figure 4d (**f**) Comparison of AIRS dust AOD (black cross), CALIOP AOD, and cloud optical depth (blue and red circle line, respectively).

From this case study, the AIRS-derived dust AODs and DTHs are in good agreement with CALIOP data. It is a very encouraging result since the training data do not cover this area. This also suggests that the local regression model could be used in an area with similar weather conditions and similar dust microphysical parameters. However, there are still additional uncertainties in retrieving dust AOD and DTH during nighttime than during daytime: when applying the statistical model based on the training data mostly from daytime too fewer nighttime cases, the results would be more influenced by atmospheric and land surface conditions.

5. Statistical Characteristics of DTHs from AIRS

The climatology of DTHs from AIRS BT measurements in the Taklimakan Desert between 2007 and 2013 are derived using the retrieval algorithm described in the previous section. Figure 7a shows the number of AIRS pixels observed in each grid with a resolution of 0.5 degree × 0.5 degree. The observed frequency of dust in the core of the desert is between 100 and 200. The highest frequency of observed dust appears in the southeastern part of the desert, and the second-highest value is in the heart of the desert. In order to ensure that there are enough samples in each grid to calculate the average value, the grids with a frequency less than 50 are excluded here. It should be noted that the results here only show the AIRS DTH retrievals under clear sky conditions.

(a)

(b)

(c)
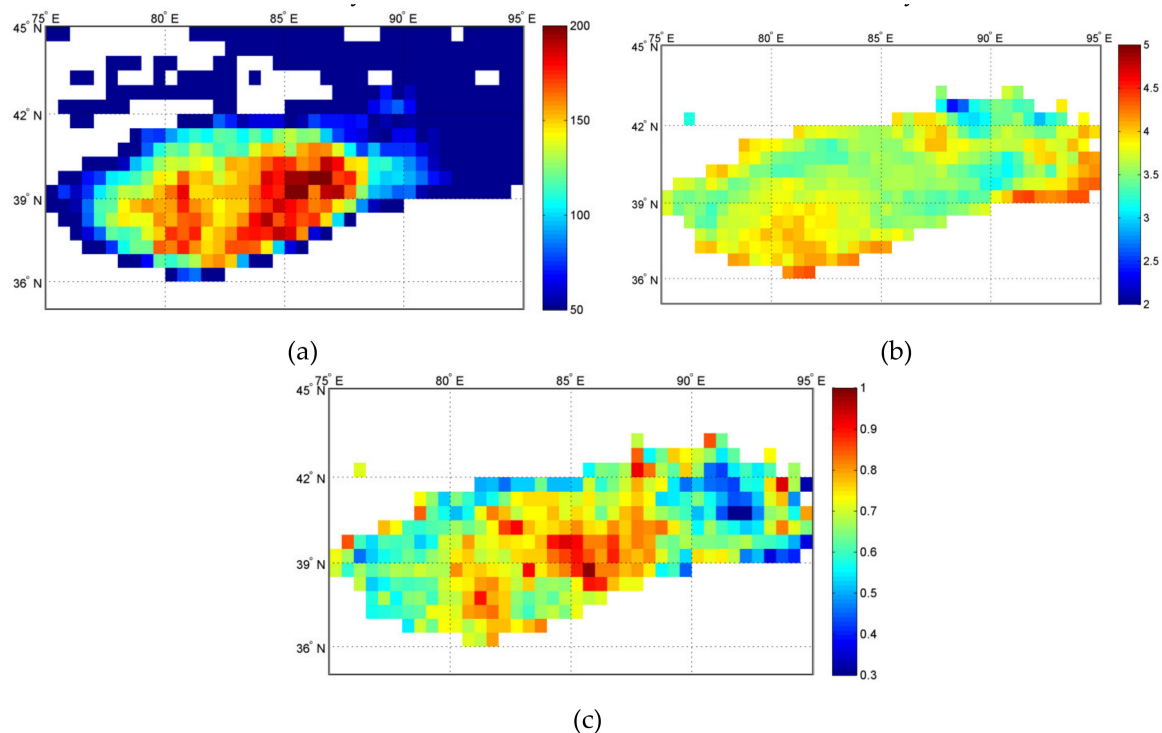
Figure 7. Statistics of the dust observations in grid with a resolution of 0.5 degree × 0.5 degree (**a**) The number of AIRS pixels observed at each grid point, (**b**) The average dust height (km) at each grid point with a maximum of 4.43 km, mean of 3.68 km, and a minimum of 2.40 km, and (**c**) The standard deviation of dust height (km) at each grid with a maximum of 0.98 km, average of 0.68 km, and a minimum of 0.26 km.

As shown in Figure 7b, the maximum of the average DTH is 4.43 km at the eastern exit and edge of the desert, which is mainly related to the direction of dust and the terrain of the basin. The minimum of the DTH is 2.40 km. The average DTH is 3.68 km.

The standard deviation (STD) of DHTs at each grid is also calculated here, ranging from 0.3 km to 1 km, as presented in Figure 7c. The high values of STD are mainly concentrated in the central to southeastern part of the desert with a maximum value of 0.98 km. The possible factors are: when the area is sandy with low transport, the DTH is relatively low; conversely, when transport is greater with dust blown from the north, the height may be relatively high. The mean of the STD is 0.68 km, and the minimum STD appears at the exit area of the eastern desert at 0.26 km.

The advantage of CALIOP is its accurate dust height information, but the limitation is that it only measures one line (nadir) and does not provide a wide range of information on the distribution of dust. AIRS has the advantage of having a wide range of observational capabilities. In this study, the retrieval algorithm is established using the collocated AIRS BT measurements and CALIOP dust heights in limited regions and is applied to AIRS BT measurements for DTH retrievals with broad coverage.

The results can be used for analysis of climatic characteristics, as the initial value for 1Dvar-based physical retrieval of dust parameters, for the numerical simulation of dust characteristics in this area, etc. The results indicate that continuous changes in the dust properties can be obtained when hyperspectral infrared instruments are onboard the geostationary weather satellites.

6. Discussions

Due to the higher emission and larger spatial variation of land compared to ocean, it is challenging to retrieve AOD values over land. To overcome these difficulties, one method involves 1Dvar-based physically retrieving the dust properties by using auxiliary data including surface emissivity and temperature, as in the previous study performed by Yao et al. [25,27]. They showed that reasonable results could be obtained by using the physical retrieval method if the surface and atmospheric information is available. Another method involves developing a local regression model by using the collocated data to reduce the impact of the variation of atmospheric and surface conditions, as well as dust composition.

Collecting eight years matched dust atmosphere data of AIRS, MODIS, and CALIOP, which are all part of A-train, the AIRS dust AOD and DTH statistic model have been developed and validated over the dust source, Taklimakan Desert. For the AOD retrieval, the validation shows the same correlation value of 0.88 with MODIS DB AOD and in-situ observation. Comparing with MODIS, the MODIS AOD presents accumulated data at a value of 4.2 and AIRS dust AOD shows it at about 0.4. This is mainly caused by the response difference at visible and infrared waveband. It should be noted that ideally the training should be done separately for daytime and nighttime since the brightness temperature (BT) differences between daytime and nighttime are large due to the surface skin temperature difference over desert [45]. Using multiple IR window channels might reduce the effects of skin temperature differences, and nighttime training is still needed when there are enough samples collected.

Based on the DTH validation results, AIRS DTHs agree well with CALIOP dust height observations. The statistical retrieval models developed in this study are independent of the dust type and atmospheric radiative transfer model (RTM), which overcomes the limitations of the physical retrieval method developed by Yao et al. [25]. For example, the accuracy of AIRS-based dust AOD and DTH using the 1Dvar-based physical retrieval method is heavily influenced by the uncertainties of the radiative transfer calculation and auxiliary data, such as atmospheric profiles and surface conditions. However, the disadvantage of the statistical method is that it strongly depends on the accuracy of the dust parameters from MODIS and CALIOP in the matchup database.

Since very few nighttime dust observations are available, only one case study for nighttime DTH and AOD retrieval using AIRS is presented in this study. Meanwhile, it is worth examining the differences between day and night for dust parameter retrievals. Considering that in northwestern China, about 30% of dust events occurred between 18:01 and 21:00 (local time) [13], other satellite data collected during the first half of the night, such as from the Infrared Atmospheric Sounding Interferometer (IASI), are needed to help analyze the properties of dust aerosols. However, currently, an IASI-based statistical retrieval model is still under development and spatial-temporal collocated observational data from an active satellite are unavailable. Another option is to use 1Dvar-based physical retrieval model to extract dust parameters IASI BT measurements.

7. Conclusions

In this paper, an AIRS-based dust AOD retrieval model has been developed using the collocated AIRS BT measurements and MODIS AOD product. Similarly, an AIRS-based DTH retrieval model is established using the collocated AIRS BT measurements and CALIOP data with an option of including MODIS DB AOD product as input for daytime cases. Through validation with independent reference data, it is demonstrated that AODs derived from AIRS are in good agreement with in-situ measurements, suggesting a potential application of the statistic retrieval model for nighttime dust AOD retrieval. With MODIS DB AOD product, AIRS DTH model shows an improved result compared

to the cases of only AIRS BTs used. The climate distribution of dust-top height is extracted based on the improved model during 2007–2013. The frequency of dust storm and mean DTH over Taklimakan Desert have been presented at a resolution of 0.5°*0.5°. The information could give support on dust atmosphere quantitative application as a reference.

The methodologies and technical approaches can be applied to the processing of global AIRS data for global dust height products over land. It can also be used to process new data such as CrIS/VIIRS from Suomi-NPP and the JPSS series, HIRAS/MERSI-II from FY-3D and its follow-on, and GIIRS/AGRI from the FengYun-4 series [28]. AIRS, together with IASI and CrIS, are able to create global dust parameters from 2002 to the present. Making full use of multi-platform satellite data will significantly improve the temporal resolution of dust parameters, which is very useful for climate studies.

Author Contributions: Conceptualization, J.L. and Z.Y.; methodology, Z.Y. and J.L.; software, Z.Y.; validation, Z.Z., L.Z., and H.C.; formal analysis, J.Q.; investigation, Z.Y.; resources, L.Z.; data curation, J.Q.; writing—original draft preparation, Z.Y.; writing—review and editing, J.L.; visualization, J.Q.; supervision, J.L.; project administration, J.Q.; funding acquisition, Z.Y. and J.Q..

Conflicts of Interest: The authors declare no conflict of interest.

References

1. Hansen, J.; Sato, M.; Ruedy, R. Radiative forcing and climate response. *J. Geophys. Res. Atmos.* **1997**, *102*, 6831–6864. [CrossRef]
2. Seinfeld, J.H.; Carmichael, G.R.; Arimoto, R.; Conant, W.C.; Brechtel, F.J.; Bates, T.S.; Cahill, T.A.; Clarke, A.D.; Doherty, S.J.; Flatau, P.J.; et al. ACE-ASIA: Regional Climatic and Atmospheric Chemical Effects of Asian Dust and Pollution. *Bull. Am. Meteorol. Soc.* **2004**, *85*, 367–380. [CrossRef]
3. Solomon, S.; Qin, D.; Manning, M.; Averyt, K.; Marquis, M.; Tignor, M.M. *Climate Change 2007-the Physical Science Basis: Working Group I Contribution to the Fourth Assessment Report of the IPCC*; Cambridge University Press: Cambridge, UK, 2007; Volume 4.
4. Yang, F.; Ali, M.; Zheng, X.; He, Q.; Yang, X.; Huo, W.; Liang, F.; Wang, S. Diurnal dynamics of soil respiration and the influencing factors for three land-cover types in the hinterland of the Taklimakan Desert, China. *J. Arid Land* **2017**, *9*, 568–579. [CrossRef]
5. Sun, J.; Zhang, M.; Liu, T. Spatial and temporal characteristics of dust storms in China and its surrounding regions, 1960-1999: Relations to source area and climate. *J. Geophys. Res. Atmos.* **2001**, *106*, 10325–10333. [CrossRef]
6. Zhuang, G.; Guo, J.; Yuan, H.; Zhao, C. The compositions, sources, and size distribution of the dust storm from China in spring of 2000 and its impact on the global environment. *Chin. Sci. Bull.* **2001**, *46*, 895–900. [CrossRef]
7. Wang, Z. Neutralization of soil aerosol and its impact on the distribution of acid rain over east Asia: Observations and model results. *J. Geophys. Res.* **2002**, *107*, 4389. [CrossRef]
8. Jickells, T.D. Global Iron Connections Between Desert Dust, Ocean Biogeochemistry, and Climate. *Science* **2005**, *308*, 67–71. [CrossRef]
9. Han, Y.; Song, L.; Zhao, T.; Zhang, Q.; Xi, X. The relationship between continental dust and marine phytoplankton in the North Pacific and its impact on marine phytoplankton. *Chin. Environ. Sci* **2006**, *26*, 157–160.
10. Eguchi, K.; Uno, I.; Yumimoto, K.; Takemura, T.; Shimizu, A.; Sugimoto, N.; Liu, Z. Trans-pacific dust transport: Integrated analysis of NASA/CALIPSO and a global aerosol transport model. *Atmos. Chem. Phys.* **2009**, *9*, 3137–3145. [CrossRef]

11. Uno, I.; Eguchi, K.; Yumimoto, K.; Takemura, T.; Shimizu, A.; Uematsu, M.; Liu, Z.; Wang, Z.; Hara, Y.; Sugimoto, N. Asian dust transported one full circuit around the globe. *Nat. Geosci.* **2009**, *2*, 557–560. [CrossRef]

12. Fischer, E.V.; Hsu, N.C.; Jaffe, D.A.; Jeong, M.-J.; Gong, S.L. A decade of dust: Asian dust and springtime aerosol load in the U.S. Pacific Northwest: A DECADE OF DUST. *Geophys. Res. Lett.* **2009**, *36*. [CrossRef]

13. Wang, S.; Wang, J.; Zhou, Z.; Shang, K. Regional characteristics of three kinds of dust storm events in China. *Atmos. Environ.* **2005**, *39*, 509–520. [CrossRef]

14. Menzel, W.P.; Schmit, T.J.; Zhang, P.; Li, J. Satellite-Based Atmospheric Infrared Sounder Development and Applications. *Bull. Am. Meteorol. Soc.* **2018**, *99*, 583–603. [CrossRef]

15. Ackerman, S.A. Remote sensing aerosols using satellite infrared observations. *J. Geophys. Res. Atmos.* **1997**, *102*, 17069–17079. [CrossRef]

16. Kaufman, Y.J.; Tanré, D.; Remer, L.A.; Vermote, E.F.; Chu, A.; Holben, B.N. Operational remote sensing of tropospheric aerosol over land from EOS moderate resolution imaging spectroradiometer. *J. Geophys. Res. Atmos.* **1997**, *102*, 17051–17067. [CrossRef]

17. Li, J.; Zhang, P.; Schmit, T.J.; Schmetz, J.; Menzel, W.P. Technical note: Quantitative monitoring of a Saharan dust event with SEVIRI on Meteosat-8. *Int. J. Remote Sens.* **2007**, *28*, 2181–2186. [CrossRef]

18. Kaufman, Y.J.; Tanré, D.; Boucher, O. A satellite view of aerosols in the climate system. *Nature* **2002**, *419*, 215–223. [CrossRef]

19. Hsu, N.C.; Tsay, S.-C.; King, M.D.; Herman, J.R. Aerosol Properties Over Bright-Reflecting Source Regions. *Ieee Trans. Geosci. Remote Sens.* **2004**, *42*, 557–569. [CrossRef]

20. Wald, A.E.; Kaufman, Y.J.; Tanré, D.; Gao, B.-C. Daytime and nighttime detection of mineral dust over desert using infrared spectral contrast. *J. Geophys. Res. Atmos.* **1998**, *103*, 32307–32313. [CrossRef]

21. Sokolik, I.N. The spectral radiative signature of wind-blown mineral dust: Implications for remote sensing in the thermal IR region. *Geophys. Res. Lett.* **2002**, *29*, 7–1–7–4. [CrossRef]

22. Pierangelo, C.; Chédin, A.; Heilliette, S.; Jacquinet-Husson, N.; Armante, R. Dust altitude and infrared optical depth from AIRS. *Atmos. Chem. Phys.* **2004**, *4*, 1813–1822. [CrossRef]

23. DeSouza-Machado, S.G.; Strow, L.L.; Hannon, S.E.; Motteler, H.E. Infrared dust spectral signatures from AIRS. *Geophys. Res. Lett.* **2006**, *33*. [CrossRef]

24. DeSouza-Machado, S.G.; Strow, L.L.; Imbiriba, B.; McCann, K.; Hoff, R.M.; Hannon, S.E.; Martins, J.V.; Tanré, D.; Deuzé, J.L.; Ducos, F.; et al. Infrared retrievals of dust using AIRS: Comparisons of optical depths and heights derived for a North African dust storm to other collocated EOS A-Train and surface observations. *J. Geophys. Res.* **2010**, *115*. [CrossRef]

25. Yao, Z.; Li, J.; Han, H.-J.; Huang, A.; Sohn, B.J.; Zhang, P. Asian dust height and infrared optical depth retrievals over land from hyperspectral longwave infrared radiances. *J. Geophys. Res. Atmos.* **2012**, *117*. [CrossRef]

26. Han, H.-J.; Sohn, B.J. Retrieving Asian dust AOT and height from hyperspectral sounder measurements: An artificial neural network approach. *J. Geophys. Res. Atmos.* **2013**, *118*, 837–845. [CrossRef]

27. Yao, Z.; Li, J.; Zhao, Z. Synergistic use of AIRS and MODIS for dust top height retrieval over land. *Adv. Atmos. Sci.* **2015**, *32*, 470–476. [CrossRef]

28. Yang, J.; Zhang, Z.; Wei, C.; Lu, F.; Guo, Q. Introducing the New Generation of Chinese Geostationary Weather Satellites, Fengyun-4. *Bull. Am. Meteorol. Soc.* **2017**, *98*, 1637–1658. [CrossRef]

29. Chahine, M.T.; Pagano, T.S.; Aumann, H.H.; Atlas, R.; Barnet, C.; Blaisdell, J.; Chen, L.; Divakarla, M.; Fetzer, E.J.; Goldberg, M.; et al. AIRS: Improving Weather Forecasting and Providing New Data on Greenhouse Gases. *Bull. Am. Meteorol. Soc.* **2006**, *87*, 911–926. [CrossRef]

30. Hsu, N.C.; Tsay, S.-C.; King, M.D.; Herman, J.R. Deep Blue Retrievals of Asian Aerosol Properties During ACE-Asia. *Ieee Trans. Geosci. Remote Sens.* **2006**, *44*, 3180–3195. [CrossRef]

31. Li, X.; Xia, X.; Wang, S.; Mao, J.; Liu, Y. Validation of MODIS and Deep Blue aerosol optical depth retrievals in an arid/semi-arid region of northwest China. *Particuology* **2012**, *10*, 132–139. [CrossRef]

32. Winker, D.M.; Hunt, W.H.; McGill, M.J. Initial performance assessment of CALIOP. *Geophys. Res. Lett.* **2007**, *34*. [CrossRef]

33. Holben, N.B.; Eck, F.T.; Slutsker, I.; Tanré, D.; Buis, P.J.; Setzer, A.; Vermote, E.; Reagan, A.J.; Kaufman, J.Y.; Nakajima, T.; et al. AERONET-a federated instrument network and data archive for aerosol characterization. *Remote Sens. Environ.* **1998**, *66*, 1–16. [CrossRef]

34. Che, H.Z.; Zhang, X.Y.; Chen, H.B.; Damiri, B.; Goloub, P.; Li, Z.Q.; Zhang, X.C.; Wei, Y.; Zhou, H.G.; Dong, F.; et al. Instrument calibration and aerosol optical depth validation of the China Aerosol Remote Sensing Network. *J. Geophys. Res.* **2009**, 114. [CrossRef]

35. Han, X.L.; Zou, X.Y.; Song, Z.J.; Fu, D.S.; Xia, X.A.; Che, H.Z. Comparison of AVHRR aerosol optical depth production against CARSNET data in China. *Atmos. Res.* **2019**, *218*, 12–24.

36. Che, H.; Zhang, X.-Y.; Xia, X.; Goloub, P.; Holben, B.; Zhao, H.; Wang, Y.; Zhang, X.-C.; Wang, H.; Blarel, L.; et al. Ground-based aerosol climatology of China: Aerosol optical depths from the China Aerosol Remote Sensing Network (CARSNET) 2002–2013. *Atmos. Chem. Phys.* **2015**, *15*, 7619–7652. [CrossRef]

37. Eck, T.F.; Holben, B.N.; Reid, J.S.; Dubovik, O.; Smirnov, A.; O'Neill, N.T.; Slutsker, I.; Kinne, S. Wavelength dependence of the optical depth of biomass burning, urban, and desert dust aerosols. *J.Geophys. Res.* **1999**, *104*, 31333–31349. [CrossRef]

38. Qin, W.; Wang, L.; Lin, A.; Zhang, M.; Bilal, M. Improving the estimation of daily aerosol optical depth and aerosol radiative effect using an optimized artificial neural network. *Remote Sens.* **2018**, *10*, 1022. [CrossRef]

39. Kolios, S.; Hatzianastassiou, N. Quantitative aerosol optical depth detection during dust outbreaks from METEOSAT imagery using an artificial neural network model. *Remote Sens.* **2019**, *11*, 1022. [CrossRef]

40. Cho, H.-M.; Nasiri, S.L.; Yang, P.; Laszlo, I.; Zhao, X. "Tom" Detection of optically thin mineral dust aerosol layers over the ocean using MODIS. *J. Atmos. Ocean. Technol.* **2013**, *30*, 896–916. [CrossRef]

41. Yao, Z.G.; Chen, H.B.; Lin, L.F. Retrieving atmospheric temperature profiles from AMSU-A data with neural networks. *Adv. Atmos. Sci.* **2005**, *22*, 606–616.

42. Peyridieu, S.; Chédin, A.; Tanré, D.; Capelle, V.; Pierangelo, C.; Lamquin, N.; Armante, R. Saharan dust infrared optical depth and altitude retrieved from AIRS: A focus over North Atlantic–comparison to MODIS and CALIPSO. *Atmos. Chem. Phys.* **2010**, *10*, 1953–1967. [CrossRef]

43. Li, J.; Menzel, W.P.; Zhang, W.; Sun, F.; Schmit, T.J.; Gurka, J.J.; Weisz, E. Synergistic Use of MODIS and AIRS in a Variational Retrieval of Cloud Parameters. *J. Appl. Meteorol.* **2004**, *43*, 1619–1634. [CrossRef]

44. Li, J.; Huang, H.-L.; Liu, C.-Y.; Yang, P.; Schmit, T.J.; Wei, H.; Weisz, E.; Guan, L.; Menzel, W.P. Retrieval of Cloud Microphysical Properties from MODIS and AIRS. *J. Appl. Meteorol.* **2005**, *44*, 1526–1543. [CrossRef]

45. Zhang, J.; Gao, S.; Chen, H.; Yu, J.; Tang, Q. Retrieval of the land surface-air temperature difference from high spatial resolution satellite observations over complex surfaces in the Tibetan Plateau. *J. Geophys. Res. Atmos.* **2015**, *120*, 8065–8079. [CrossRef]